Synthesis of Poly(*N*-isopropylacrylamide) Under Atmospheric Pressure Plasma Conditions

Delia Spridon, Lavinia Curecheriu, Marius Dobromir, Nicoleta Dumitrascu

Faculty of Physics, "Alexandru Ioan Cuza" University of Iasi, 700506 Iasi, Romania

Received 6 May 2011; accepted 19 July 2011
DOI 10.1002/app.35280
Published online 26 October 2011 in Wiley Online Library (wileyonlinelibrary.com).

ABSTRACT: This work is focused on obtaining and characterizing thin films of a certain thermosensitive polymer, i.e., poly(*N*-isopropylacrylamide). To obtain such polymers dielectric barrier discharge plasma working at atmospheric pressure in plan–plan geometry was used. The plasma parameters were monitored during polymerization reaction by its electrical and optical signals. The obtained films were analyzed by different techniques such as X-photoelectron spectroscopy, Fourier transform infrared spectroscopy, atomic force microscopy, contact angle, impedance spectroscopy measurements, and light interferometry for thickness measurements. Chemical analyses of obtained films showed that they sort well with the polymers obtained by other methods in literature. It has been proved that plasma polymerized films have a superhydrophilic character at room temperature, the measured contact angle being around 13°, the lower critical solution temperature was also identified at about 30–31°C. The films' thickness for a 10-min duration deposition was 400 nm. © 2011 Wiley Periodicals, Inc. J Appl Polym Sci 124: 2377–2382, 2012

Key words: "smart" polymers; poly(*N*-isopropylacrylamide); atmospheric pressure plasma; plasma polymerization

INTRODUCTION

"Smart" surfaces are recognized as valuable materials for biomedical applications. The importance of these surfaces is due to their special properties to respond to external stimuli, such as temperature, pH, electrical or magnetic field, radiation etc.[1–4] Poly (*N*-isopropylacrylamide), (pNIPAM) is termosensitive polymer, extensively studied due to its fast response to the temperature variations. The chain conformation of pNIPAM films changes along with temperature fluctuations, followed by surface modifications of the wettability and its chemistry.[5] Because both of these surface properties affect protein behavior, the amount of adsorbed proteins varies when the temperature of the polymer is higher or smaller than its lower critical solution temperature (LCST).[5,6] The ability to change surface properties by adjusting temperature made pNIPAM-based polymers to be exploited in a wide range of applications, including cell culture,[7,8] scaffold for tissue engineering,[9] filtration biomembranes,[10,11] medical diagnostic, or controlled drug delivery.[12–14]

There are various methods to obtain pNIPAM: chemical reactions based on different mechanisms such as atom transfer radical polymerization,[15] redox initiating polymerization, gamma, UV radiation,[16,17] and electron-beam induced polymerization,[18,19] and polymerization under the plasma conditions.[20]

The aim of our work is to characterize pNIPAM films obtained using a new technique based on atmospheric pressure plasma. Short deposition times, various kinds of substrates that can be used, and the low cost, are the main advantages of the atmospheric pressure plasma polymerization. Other advantages are related to high degree of reticulation and thickness control at nanoscale of plasma-polymerized films which can be optimized by changing the plasma parameters. However, the main drawback of this technique is the low deposition rate so that we can obtained only thin polymeric films.

These films will be used for certain biomedical applications such as substrate for controlled protein/drugs immobilization or biomembranes.

EXPERIMENTAL

Materials

N-isopropylacylamide monomer was used from Sigma Aldrich with 97% purity and it was heated to 70°C for an easier vaporization. The substrates for pNIPAM films were poly(ethylene terephthalate) (PET) films (GoodFellow) three times sonicated in ethanol, and KBr discs for FTIR analysis which were

Correspondence to: D. Spridon (dspridon@plasma.uaic.ro) or N. Dumitrascu (nicoleta.dumitrascu@uaic.ro).

Contract grant sponsor: European Social Fund; contract grant numbers: POSDRU/88/1.5/S/47646, POSDRU/89/1.5/S/49944.

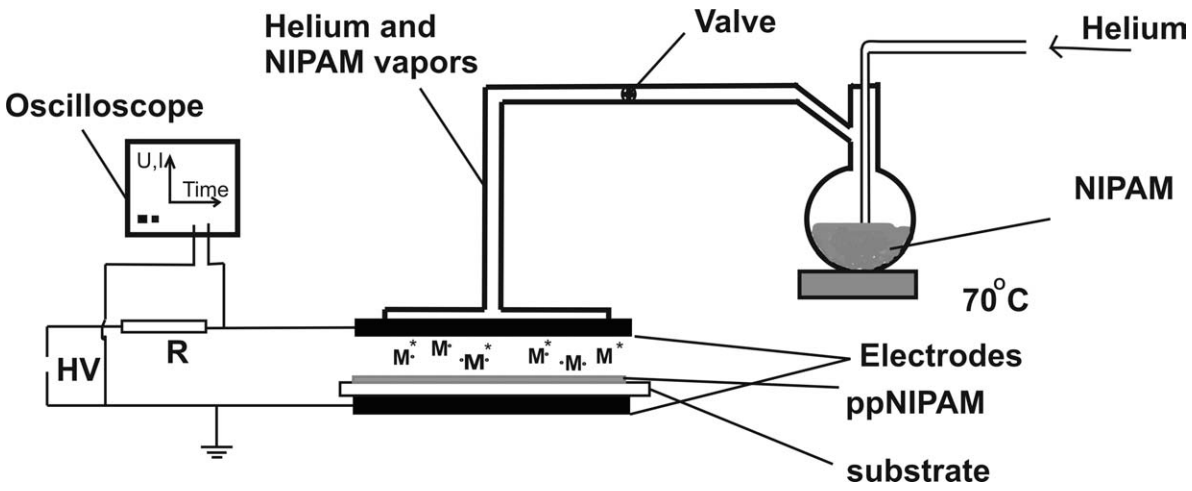

Figure 1 Experimental setup.

cleaned and dried at 50°C. Formamide from Sigma Aldrich and bidistilled water were used for contact angle measurements.

Procedure

To deposit pNIPAM onto the above substrates atmospheric pressure plasma (APP) was used as energetic medium to initiate polymerization reaction.[21,22] The APP was generated in dielectric barrier discharge in plan–plan geometry using a high tension source (Trek PD07016) and a function generator (Tabor Electronics WW5064). The dielectric barrier was glass and as working gas helium was used with 99.999% spectral purity (Fig. 1). The helium and the monomer flow rates were 3 L min^{-1} and 5 μg min^{-1}, respectively. The duration of plasma polymer deposition onto the substrate was 10 min.

The APP was monitored during processing, i.e., in pure helium and mixture of helium and NIPAM vapors. The applied voltage and the discharge current were recorded using a digital oscilloscope (TDS5034, Tektronix). Voltage measurements were performed using a voltage divider (1000 : 1 ratio), and a 150-Ω resistor was used for discharge current measurements. Time evolution of the discharge current for a maximum of sinusoidal tension 4 kV, 3 L min^{-1} helium flow rate, and 5-mm electrodes gap length is shown in Figure 2.

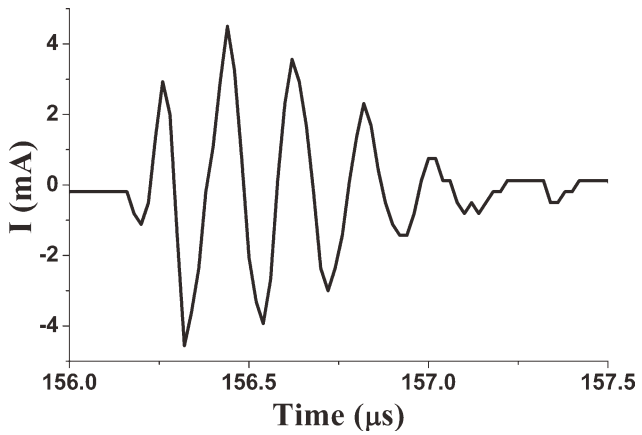

Figure 2 Time evolution of discharge current; 4 kV maximum of sinusoidal tension, 3 L min^{-1} helium flow rate, and 5-mm electrodes gap length.

Optical emission spectra of the APP were recorded with an optical fiber and then analyzed with a monochromator (Triax 550) with CCD detector (Symphony). Low and high resolution spectra of "pure" helium and mixture of helium and NIPAM vapors plasmas were taken between 200 and 900 nm.

Experimental techniques

The obtained plasma polymerized NIPAM (ppNIPAM) films were analyzed by different techniques such as Fourier transform infrared spectroscopy (FTIR), X-photoelectron spectroscopy (XPS), contact angle (CA), atomic force microscopy (AFM), impedance spectroscopy (IS).

To identify the chemical composition of obtained polymer, XPS analysis was carried out on a PHI 5000 VersaProbe X-ray photoelectron spectrometer with 0.8 eV resolution and for FTIR measurements Bomem MB-104 spectrometer was used with 0.1 cm^{-1} resolution. The measurements were made at room temperature and controlled humidity conditions.

TABLE I
Dispersive (γ_l^d) and Polar (γ_l^p) Components of Test Liquids Surface Energy

Test liquid	γ_l^d (mN m^{-1})	γ_l^p (mN m^{-1})
Bidistilled water	21.8	51
Formamide	39.5	18.7

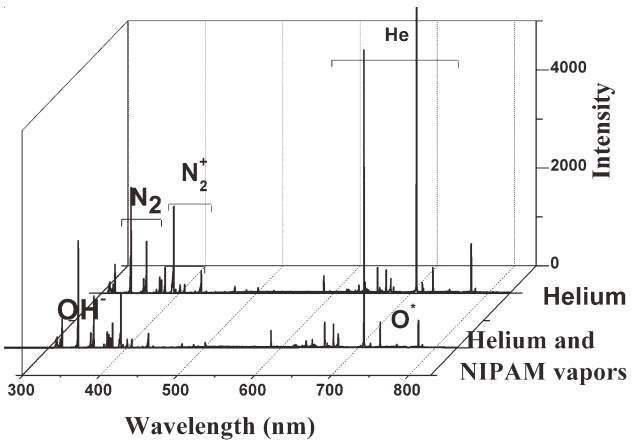

Figure 3 Spectral diagnosis of the APP in helium and mixture of helium and NIPAM vapors.

The thickness of obtained films was evaluated by light interferometry, a fast and low-cost technique with a precision of ± 50 nm.

For CA measurements we utilized an optical system, with a photo camera and a telescope with 20× magnification. The CA measurements were made with drops of 1 μL volume and the temperature of the probe was externally controlled in the range 15–55°C. Drops' photos were digitized and analyzed with the ImageJ program. There were 10 contact angles measured onto three different probes for each temperature. The presented results are averaged values of measured contact angle and the mean standard deviation is ±1°. Also, using CA measurements the surface energy components of obtained polymers were calculated at room temperature. We used two test liquids with known energetic components, i.e., water and formamide, and the Owens şi Kaelble method to calculate surface energy

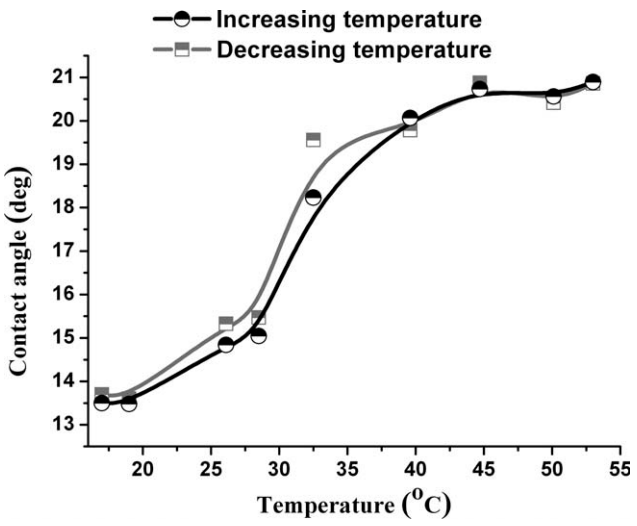

Figure 4 Temperature dependence of water contact angle onto ppNIPAM films.

TABLE II
Surface Energy Dispersive (γ_s^d) and Polar (γ_s^p) Components and Polarity of the ppNIPAM and PET Substrate Films

	γ_s^d (mN m^{-1})	γ_s^p (mN m^{-1})	P
PET	39.4	3.9	0.09
ppNIPAM	32.5	14.5	0.3

dispersive and polar components.[23,24] The energetic characteristics of the test liquids are presented in Table I.

The polarity of the surface was estimated with the below relation:

$$P = \frac{\gamma_s^p}{\gamma_s^p + \gamma_s^d}$$

where P is surface polarity, γ_s^p and γ_s^d are the polar and dispersive components of surface energy.

The dielectric properties of the ppNIPAM films have been determined at room temperature using the IS technique working in the frequency range of 10^1–10^6 Hz. The measurements were performed with a Solartron 1260A impedance spectroscopy system using an electrode kit with two plates with adjustable thickness. The applied voltage was 0.1 V and the diameter of the electrodes 2 cm.

The sample morphologies were visualized and compared by atomic force microscope (Solver Pro NT-MDT), working in tapping mode, with commercial standard silicon nitride cantilever NSC01 and tips radius ≤10 nm. The AFM resolution is 10 nm for XY and 3 nm for Z. Five different areas of each sample with dimensions from 30 μm × 30 μm to 3 μm × 3 μm were scanned, with the aim of studying the surface morphological details from micro to nano scale. The scans were made at room temperature.

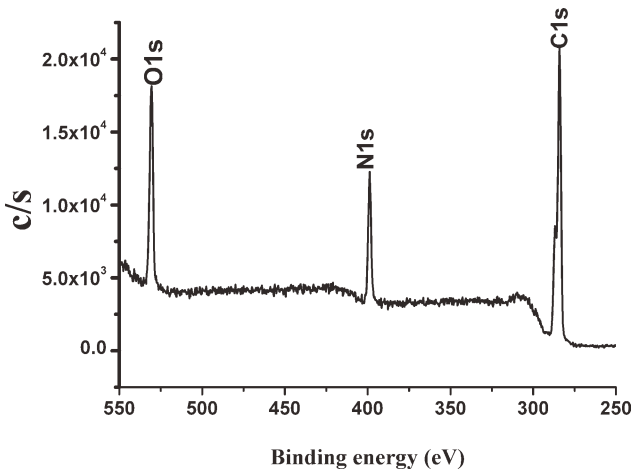

Figure 5 XPS spectra of ppNIPAM film.

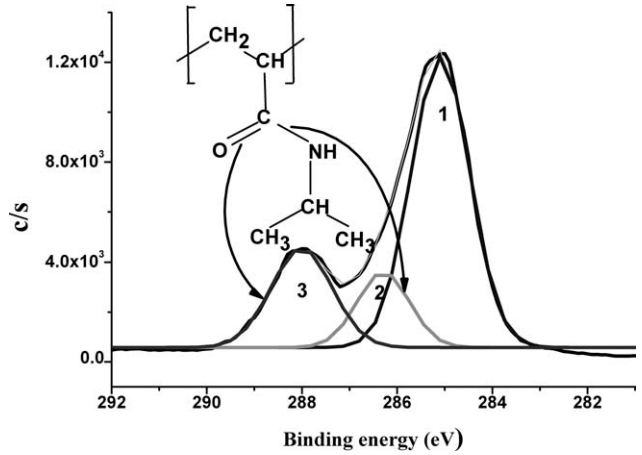

Figure 6 XPS high resolution spectrum of C 1s in ppNIPAM film.

RESULTS AND DISCUSSIONS

Spectral analysis of APP

The spectral diagnosis of the discharge (Fig. 3) shows the presence of excited species of N_2 (315.9, 337.1, and 357.6 nm), the N_2^+ molecules (391.4, 427.8, and 470 nm), hydroxyl group (308.9 nm). Also, there can be observed excited atomic oxygen lines (777.4 and 844.6 nm), from the air and the helium lines (388.1, 501.5, 587.5, 667.8, and 706.5 nm). When the monomer is introduced into the discharge, the intensity of all the aforementioned lines decreased because of the energy loss of plasma particles breaking the monomer molecules.

Small values of discharge current, maximum 4 mA in our experiments (Fig. 2), proved that helium metastable-excited species can be the main energies responsive for monomer fragmentation and not due to thermal heating of macromolecules.

Using the plasma conditions mentioned above the average thickness of polymer films was 400 nm for 10-min duration of polymerization. The film deposition was uniform with almost constant thickness onto the entire deposited surface.

Contact angle

The thermosensitivity of the plasma polymers can be proved easily by CA measurements. Using the contact angle dependence on temperature (Fig. 4) the LCST was found in a small range, around 30–31°C. Related to the superhydrophilic character of the obtained films the measured contact angle was of 13.5° at room temperature. Increasing the substrate temperature, there takes place a phase transition at LCST and the contact angle increases to 20°–21°. It was also proved that the thermosensibility is reversible as it is shown in the Figure 4.

Comparing with literature results,[12,13,25] the ppNIPAM film obtained by us is more hydrophilic, probably because of the permanent contact of the polymer with plasma.

In Table II are presented the surface energetic components. As it can be seen the value of ppNIPAM polar component is higher as compared with the PET film used as substrate.

The aging of ppNIPAM measured after 1 month from film synthesis, proved also the time stability of the plasma polymerized films.

TABLE III
Elemental Composition (Atomic %) of ppNIPAM and pNIPAM from XPS Spectra

	C	O	N
ppNIPAM	53%	30%	17%
pNIPAM	75%	12.5%	12.5%

TABLE IV
C Bond Distribution of ppNIPAM from High Resolution XPS Spectra and C Bond Distribution of pNIPAM

	C—C, C—H	C=O	C—N
ppNIPAM	56.8%	25.8%	17.4%
pNIPAM	66.7%	16.7%	16.7%

Chemical composition

The XPS survey spectra of ppNIPAM are shown in Figure 5. Three main peaks are observed, respectively, carbon at 285 eV, nitrogen at 400 eV, and oxygen at 531 eV, corresponding to the chemical composition of obtained polymer. By comparison, the percentage of chemical elements in ppNIPAM and classical pNIPAM are presented in Table III, excluding hydrogen. We identified an increased content of oxygen and nitrogen in composition of

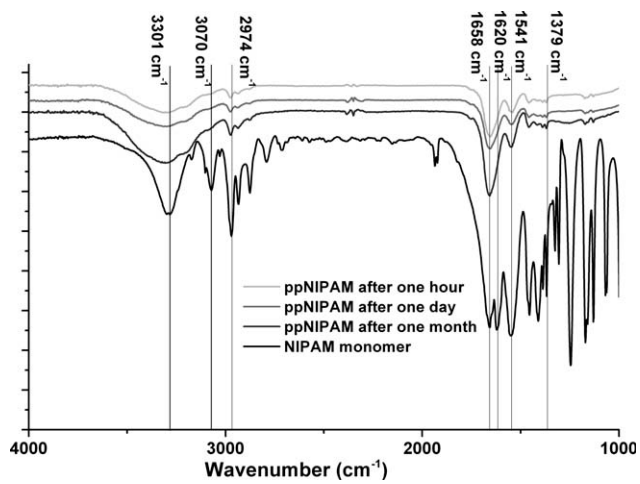

Figure 7 FTIR spectra of monomer and ppNIPAM film.

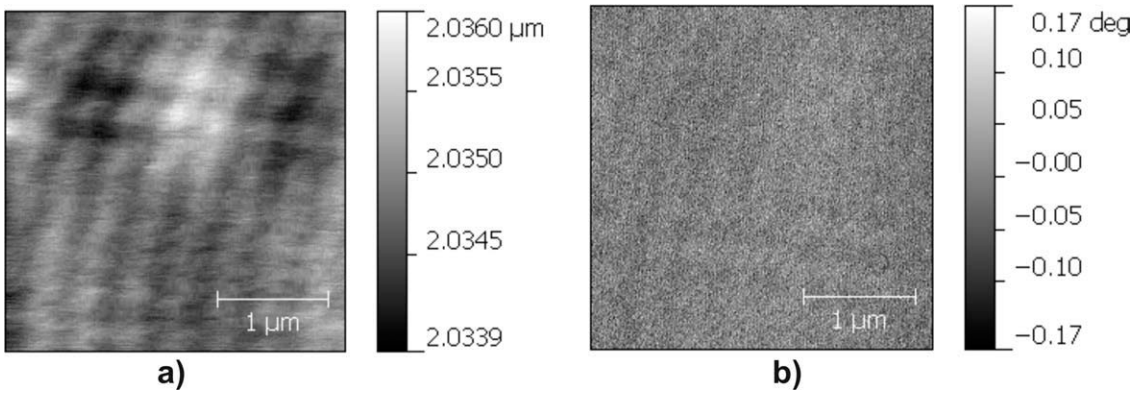

Figure 8 AFM images: topography (a) and phase image (b) of ppNIPAM films.

plasma polymerized films as against pNIPAM is due to the atmospheric pressure plasma conditions.

Additional information on the molecular structure of ppNIPAM was obtained from the XPS high-resolution C 1s scan, three peaks with approximately the same width (1.2 eV). Thus, the fitted peaks are shown in Figure 6, corresponding to the carbons, C—C and C—H, at 285.0 eV,[1] to C—N at 286.1 eV,[2] and the C=O bond at 287.8 eV.[3] From the quantitative evaluation of XPS signal the carbons are distributed in ppNIPAM as follows: 56.8% of carbons are in C—C and C—H, 17.4% are implicated in C—N bonds, and 25.8% are C=O bonds. If we compare the C bonds distribution in our ppNIPAM with classical pNIPAM film[9] we observe that in plasma polymerized films there are more C=O and C—N bonds, also due to experimental conditions, i.e., atmospheric pressure plasma (Table IV).

The FTIR spectra of monomer and ppNIPAM are shown in Figure 7. Thus, the peak assignments are as follows: the 1379 cm^{-1} band is attributed to the deformation of two methyl groups on the isopropyl [—$CH(CH_3)_2$] functionality, 1541 cm^{-1} to secondary amide *N*—H stretching, aka amide II band. Also 1658 cm^{-1} band corresponds to secondary amide C=O stretching, aka amide I band, 2974 cm^{-1} to —CH_3 asymmetric stretching; 3070 cm^{-1} to amide II band overtone; and 3301 cm^{-1} to secondary amide *N*—H stretching. As shown in the Figure 7 the C=C bond absorption band observed near 1620 cm^{-1} of the pure monomer disappeared in polymer spectrum; this result being similar to XPS results where the double bond was not identified (Fig. 6).

As it can be seen in the FTIR spectra (Fig. 7) time evolution of ppNIPAM spectra proved their stability, the main bands being the same after 1 week from the synthesis.

Surface morphology

AFM images show very smooth ppNIPAM surface [Fig. 8(a)], the root mean square roughness being around 0.2 nm for a 3 µm × 3 µm image. Moreover, from chemical point of view, the obtained film is uniform as can be seen from phase image [Fig. 8(b)] of AFM.

Impedance spectroscopy

The dielectric response of the polymers yield certain information about the motion of molecular chains and relaxation processes. The large frequency range (10–10^6 Hz), over which the dielectric characteristic of polymer were studied, made possible to correlate the observed dielectric response to slow or fast molecular events.[26]

The frequency dependence of the real part of permittivity Re(ε), and dielectric loss tan δ, of PET substrate, and PET coated with ppNIPAM films at room temperature is shown in Figure 9. Thus, the permittivity values of PET films sort well with that obtained elsewhere.[27]

Related to the sandwich sample composed by ppNIPAM and PET, it is observed a permittivity up to 6 in the low frequency domain (1–100 Hz),

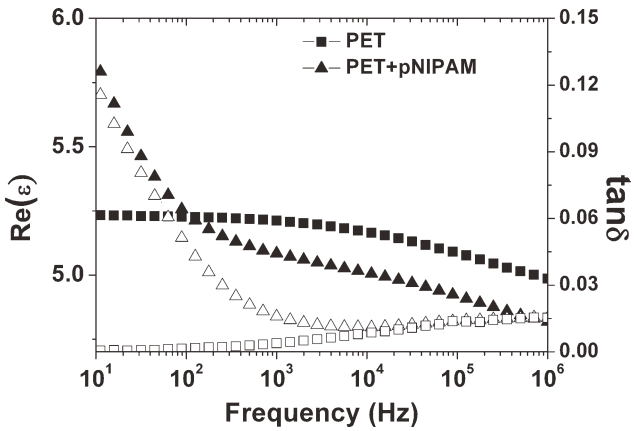

Figure 9 Frequency dependence of the dielectric properties of PET substrate and PET coated with ppNIPAM: real part of electrical permittivity, Re(ε) and dielectric loss tan δ.

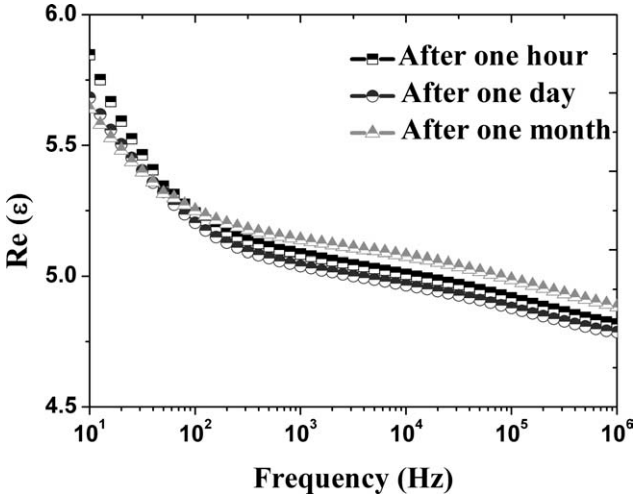

Figure 10 Aging of dielectric constant of ppNIPAM-coated PET films.

decreasing down to 4.6, at higher frequencies (Fig. 9). This dipolar relaxation phenomenon is probably due to oxygen absorption into the ppNIPAM matrix during polymerization process. This opinion is sustained by XPS analysis that shows an increased oxygen in the polymer composition (Fig. 6).

Also, it can be observed that the samples are good dielectrics with low losses at all frequency ($\tan \delta < 0.12$) (Fig. 9). The higher values of $\tan \delta$ at low frequencies may be attributed to the higher polarity which induces an increased surface conductivity of ppNIPAM film (Table II).

Investigation of dielectric properties stability given the same conclusion, respectively, the electrical properties of ppNIPAM films are stable in time (Fig. 10).

CONCLUSIONS

Polymerization of NIPAM monomers has been carried out using a new technique based on atmospheric pressure plasma in a mixture of helium and its vapors. This technique has important advantages over the methods reported to obtain ppNIPAM films onto solid supports. Using short duration of polymerization it obtained thin uniform polymeric films having a superhydrophilic character and good time stability. The chemical composition is proved by XPS and FTIR analysis and they are in good agreement with the polymer obtained by known methods. The temperature responsiveness of the coating has been observed by contact angle measurements and the LCST was identified. The impedance spectroscopy analysis proved also the time stability of dielectric properties of our films.

Our APP plasma can be of practical interest because of simplicity of experimental setup, more, it is working at atmospheric pressure, without vacuum devices, a low expensive method. The above properties, including control of the thickness at nanoscale and high degree of reticulation of films can be easily modified by changing the plasma parameters as depending on the application.

We intend to use these plasma polymer films for certain biomedical applications such as substrate for controlled protein/drugs immobilization or biomembranes.

References

1. Imran, A. B.; Seki, T.; Takeoka, Y. Polym J 2010, 42, 839.
2. Aguilar, M. R.; Elvira, C.; Gallardo, A.; Vázquez, B.; Roman, J. S. E-book: Topics in Tissue Engineering; Ashammakhi, N., Reis, R. L., Chiellini, E., Eds.; 2007; Vol. 3, Chapter 6, pg 1–27.
3. Kumara, A.; Srivastava, A.; Galaev, I. Y.; Mattiasson, B. Prog Polym Sci 2007, 32, 1205.
4. Ulijn, R. V.; Bibi, N.; Jayawarna, V.; Thornton, P. D.; Todd, S. J.; Mart, R. J.; Smith, A. M.; Gough, J. E. Materials 2007, 10, 40.
5. Plunkett, K. N.; Zhu, X.; Moore, J. S.; Leckband, D. E. Langmuir 2006, 22, 4259.
6. Yim, H.; Kent, M. S.; Huber, D. L. Macromolecules 2003, 36, 5244.
7. Cheng, X.; Wang, Y.; Hanein, Y.; Bohringer, K. F.; Ratner, B. D. J Biomed Mater Res A 2004, 70, 159.
8. Ohya, S.; Kidoaki, S.; Matsuda, T. Biomaterials 2005, 26, 3105.
9. Klouda, L.; Mikos, A. G. Eur J Pharm Biopharm 2008, 68, 34.
10. Peng, T.; Cheng, Y. L. J Appl Polym Sci 1998, 70, 2133.
11. Lue, S. J.; Hsu, J. J.; Chen, C. H.; Chen, B. C. J Membr Sci 2007, 301, 142.
12. Nagel, B.; Warsinke, A.; Katterle, M. Langmuir 2007, 23, 6807.
13. Ying, L.; Kang, E. T.; Neoh, K. G.; Kato, K.; Iwata, H. J Membr Sci 2004, 243, 253.
14. Ista, L. K.; Lopez, G. P. J Ind Microbiol Biot 1998, 20, 121.
15. Lu, X.; Zhang, L.; Meng, L.; Liu, Y. Polym Bull 2007, 59, 195.
16. Kubota, H.; Nagaoka, N.; Katakai, R.; Yoshida, M.; Omichi, H.; Hata, Y. J Appl Polym Sci 1994, 51, 925.
17. Okano, T.; Yamada, N.; Okuhara, M.; Sakai, H.; Sakurai, Y. Biomaterials 1995, 16, 297.
18. Peng, T.; Chen, Y. L. J Appl Polym Sci 1998, 70, 2133.
19. Kanazawa, H.; Yamamoto, K.; Matsushima, Y.; Takai, N.; Kikuchi, A.; Sakurai, Y.; Okano, T. Anal Chem 1996, 68, 100.
20. Pan, Y. V.; Wesley, R. A.; Luginbuhl, R.; Denton, D. D.; Ratner, B. D. Biomacromolecules 2001, 2, 32.
21. Yasuda, H. Plasma polymerization. Academic Press: New York, 1985.
22. Morent, R.; De Geyter, N.; Trentesaux, M.; Gengembre, L.; Dubruel, P.; Leys, C.; Payen, E. Appl Surf Sci 2010, 257, 372.
23. Owens, D. K.; Wendt, R. C. J Appl Polym Sci 1969, 13, 1741.
24. Kaelble, D. H.; Uy, K. C. J Adhes 1970, 2, 50.
25. Wang, Y. P.; Kun Yuan, T.; Li, Q. L.; Wang, L. P.; Gu, S. J.; Pei, X. W. Mater Lett 2005, 59, 1736.
26. Mijovic, J.; Fitz, B. D. Novocontrol: Application Notes 2; 1998 www.novocontrol.de/pdf_s/APND2.PDF.
27. Svorcik, V.; Ekrt, O.; Rybka, V.; Liptak, J.; Hnatowicz, V. J Mater Sci Lett 2000, 19, 1843.